

The New World of Impact Cratering: The High-Resolution Digital Terrain Model and Hydrocode Modeling – The Saarland (Germany) Low Altitude Touchdown Airburst Impact Event

The New World of Impact Cratering: The High-Resolution Digital Terrain Model and Hydrocode Modeling – The Saarland (Germany) Low Altitude Touchdown Airburst Impact Event

Kord Ernstson¹, Werner Müller², Andreas Gawlik-Wagner³ and Allen West⁴,
¹University of Würzburg, 97074 Würzburg (Germany) kernstson@ernstson.de, ²Diefflerstraße 217, 66809 Nalbach (Germany), ³Antoniusweg 3, 66763 Dillingen (Germany), ⁴Comet Research Group, Prescott, Arizona 86301, USA.

Introduction

In impact research, the term impact cratering generally refers to the impact of cosmic bodies (asteroids, comets) that create a correspondingly more or less large/deep crater. More recently, this view has been expanded to include the assumption that a comparatively large number of impacts have

Primary and secondary Impacts

Primary Impacts

In impact cratering, the term secondary impact is used when (primary) ejecta, which have been hurled out of high energy, cosmic (secondary) impact craters when they land.

Primary and secondary Impacts

Butterfly Impacts

Often, the impact structures have a kind of butterfly shape, which, although in very different sizes, are related to structures on Mars and at the Tunguska airburst impact (Figs. 6, 7). In the case of the Tunguska airburst, the geometrically similar shape is striking (Fig. 7), which indicates a similar energy distribution across the entire area.

The Saarland Impact

Thanks to investigations and numerical analyses conducted here, we have been able to determine the impact event and its location. The impact structure is located in the Saarland region, near the border of Germany and France. The impact event is dated to the year 10,000 BC. The impact structure is located in the Saarland region, near the border of Germany and France. The impact event is dated to the year 10,000 BC.

Discussion

With the routine application of the extremely high-resolution digital terrain model (DTM), impact research has entered a new phase. What we have already referred to as an obvious paradigm shift (Ernstson et al. 2024 [5]) has hardly been adopted in traditional impact research or is deliberately ignored, which is not discussed here. As can be seen from the title, this development also applies to new findings on low-altitude touchdown airburst impacts, whereby there is undoubtedly a fruitful

Kord Ernstson¹, Werner Müller², Andreas Gawlik-Wagner³ and Allen West⁴,

¹University of Würzburg, 97074 Würzburg (Germany) kernstson@ernstson.de, ²Diefflerstraße 217, 66809 Nalbach (Germany), ³Antoniusweg 3, 66763 Dillingen (Germany), ⁴Comet Research Group, Prescott, Arizona 86301, USA.



PRESENTED AT:



INTRODUCTION

In impact research, the term impact cratering generally refers to the impact of cosmic bodies (asteroids, comets) that create a correspondingly more or less large/deep crater. More recently, this view has been expanded to include the assumption that a comparatively large number of impacts have occurred in the form of low-altitude touchdown airburst impacts. The reason for this is that digital terrain models of the earth's surface at the highest resolution detect impacts with previously unknown precision, most notably when they have left unmistakable traces, especially in the more recent and most recent geological times of the Pleistocene and Holocene. Here, we present an example that impressively demonstrates this new perspective and research direction.

The Digital Terrain Model

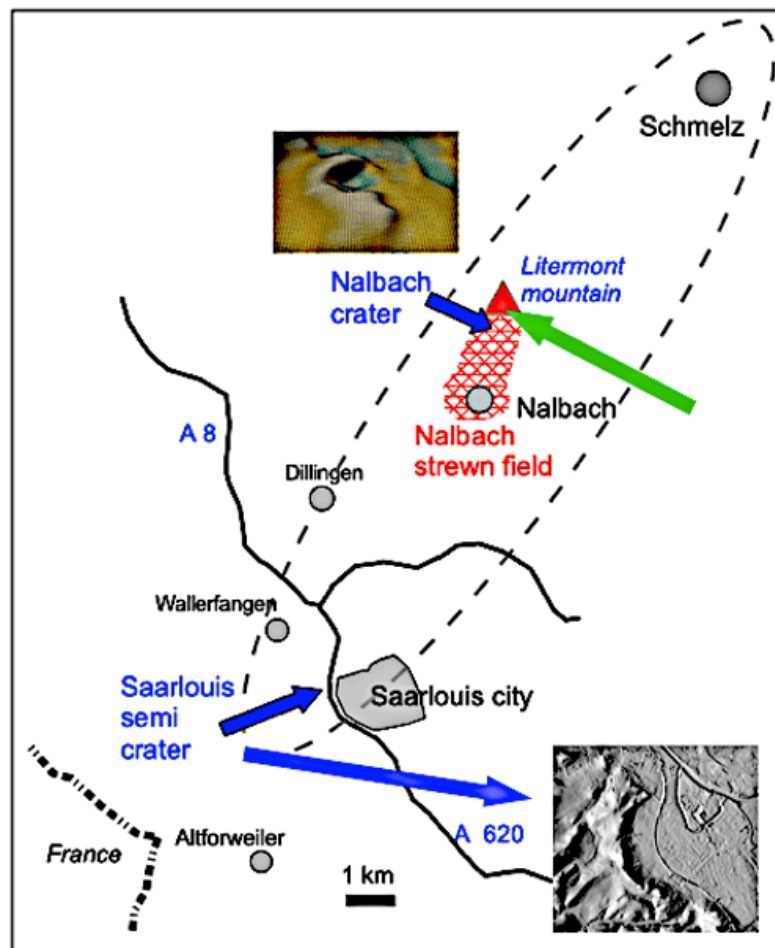
: The Digital Terrain Model DTM is a relatively new representation of the topography of the earth's surface with a dense data network obtained from LASER scanning from an airplane. The DTM data used here for a 1 m x 1 m grid at a vertical resolution of 10 cm with interpolation down to the decimeter and centimeter range, capture the bare ground without buildings and vegetation, even in dense forests and swamps.

Hydrocode Modeling

Hydrocodes are computer programs that model the response of materials to extremely short-term loading, while a more accurate description is shock wave physics code. It describes the flow behavior of solid materials at velocities much greater than the materials local sound (seismic) velocity. Modern hydrocodes model both hydrodynamic and material effects like rock strength and fracturing.

Terrain investigations and material analyses evolved into what is now called the Saarland impact and now includes two 250 m-diameter (Nalbach) and 2.3 km-diameter (Saarlouis) craters (Ernstson et al. 2013, 2018).

A map of Germany with four red dots marking the locations of Köln, Berlin, Saarbrücken, and München. A black arrow points to Saarbrücken, with the text 'Saarland impact' written in blue next to it. A scale bar indicates 100 km. An inset map in the top right corner shows the location of Germany within Europe, with a black arrow pointing to Germany.



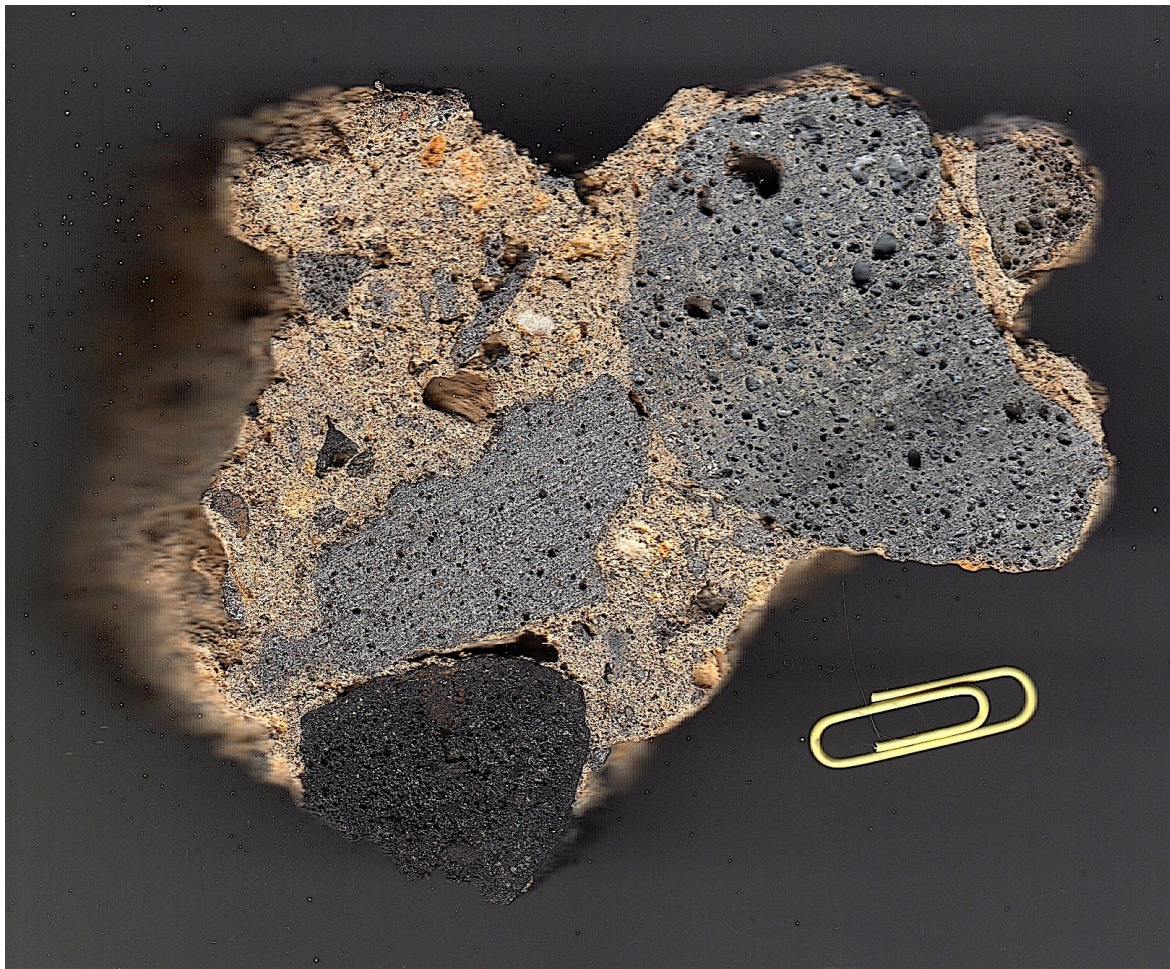
Location map; area addressed here, green arrow.

Impact evidence is the widespread strong shock effects (shock metamorphism like quartz PDFs, PFs, diaplectic glass, mica kink banding, SiO₂ ballen structures, toasted quartz, spallation fractures) detected in impactites, which hence comprise virtually all evidence recorded in impact research. Shatter cones in quartzite rocks add to the clear impact shock evidence (Siegel et al. 2023). The occurrence and distribution of the impact rocks and impact glasses with over an area of more than 10 km directly on the surface or at a depth of 20-30 cm has already led to the conclusion of a young Holocene touchdown airburst impact, which will be further specified.

Impact rocks and shock metamorphism

(small selection of a very large Saarland impact collection)

Suevites, polymictic breccias, breccia generations











Impact melt rocks and glasses



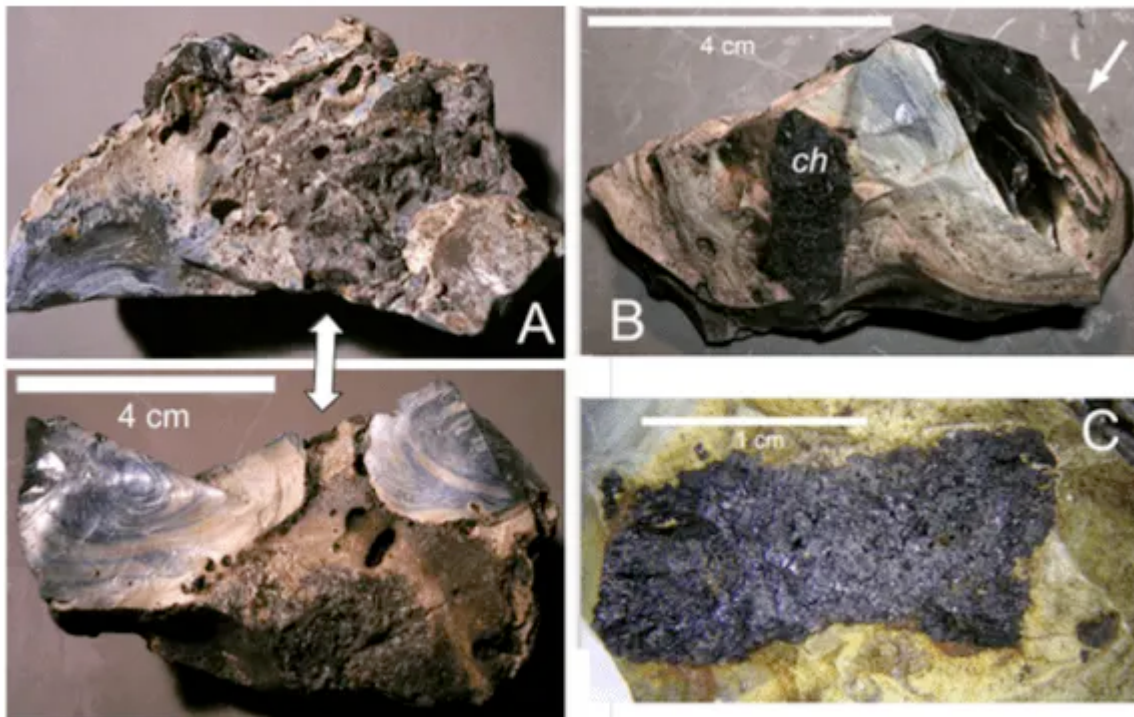
Bone fragments in black impact glass.



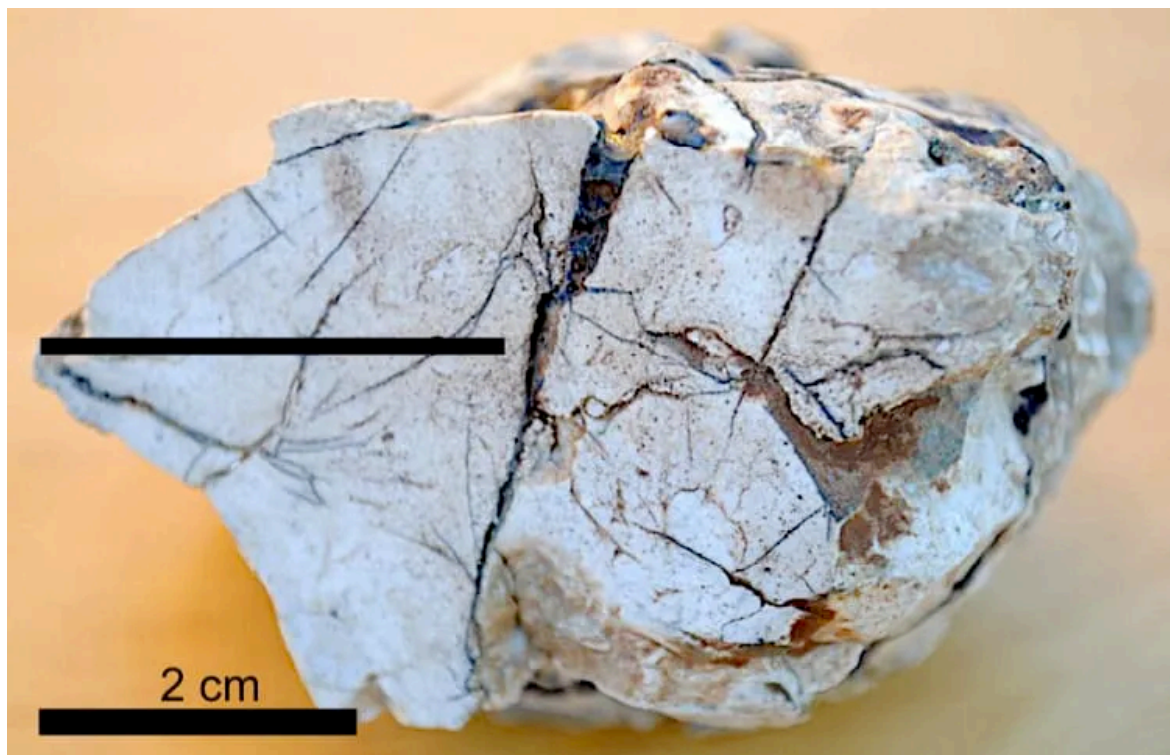
Massive black glass chunk with a vesicular, in part polymictic melt rock shell with structures reminding of volcanic Pahoehoe lava flow.



Similar chunk of black glass wrapped round by partly melted sedimentary (reddish Buntsandstein) rock.



Polymictic vesicular melt breccia (front and rear) with coiled globular bluish glass components. B, C: Polymictic melt rock with brownish-olive glass in sharp contact with bluish glass. ch = a freshly broken chiemite component.



Quartzite cobble enveloped in glass skin and glass-filled shock spallation fractures.



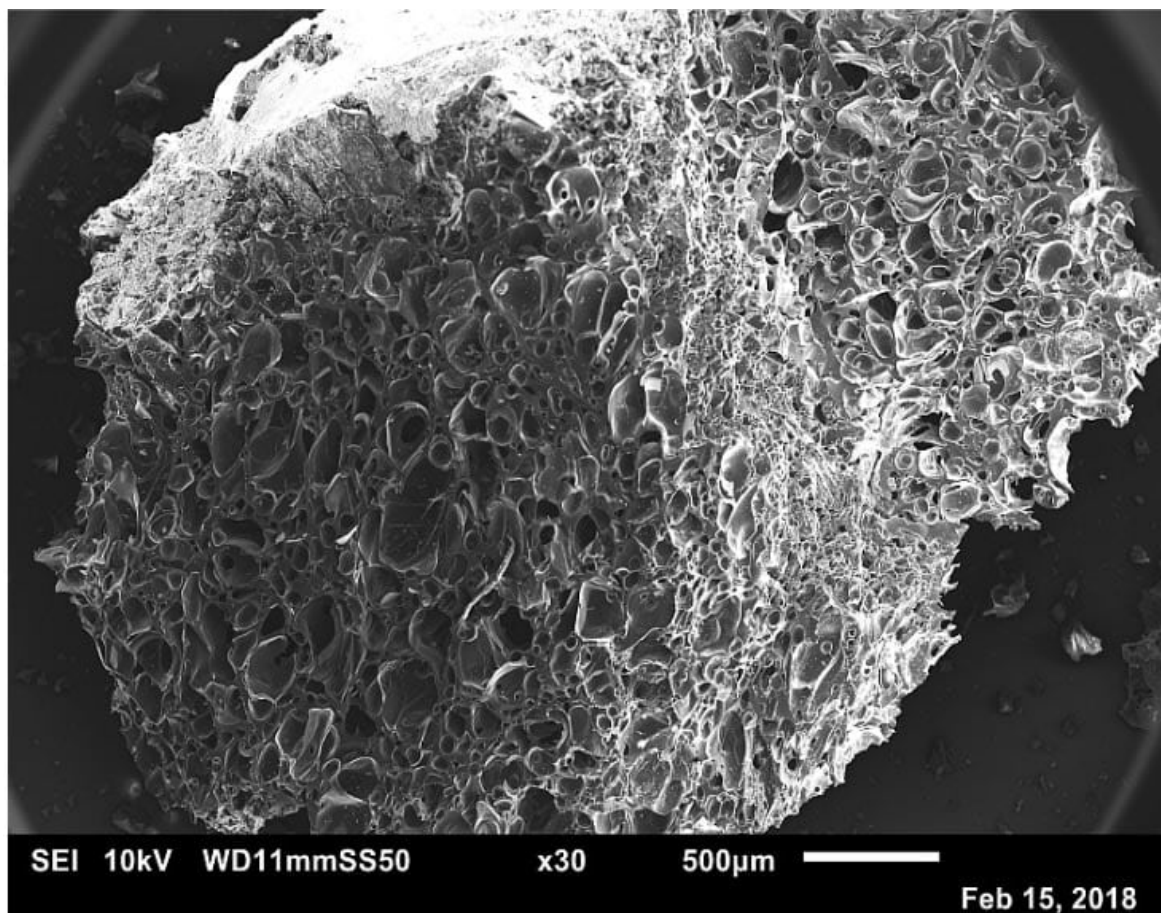
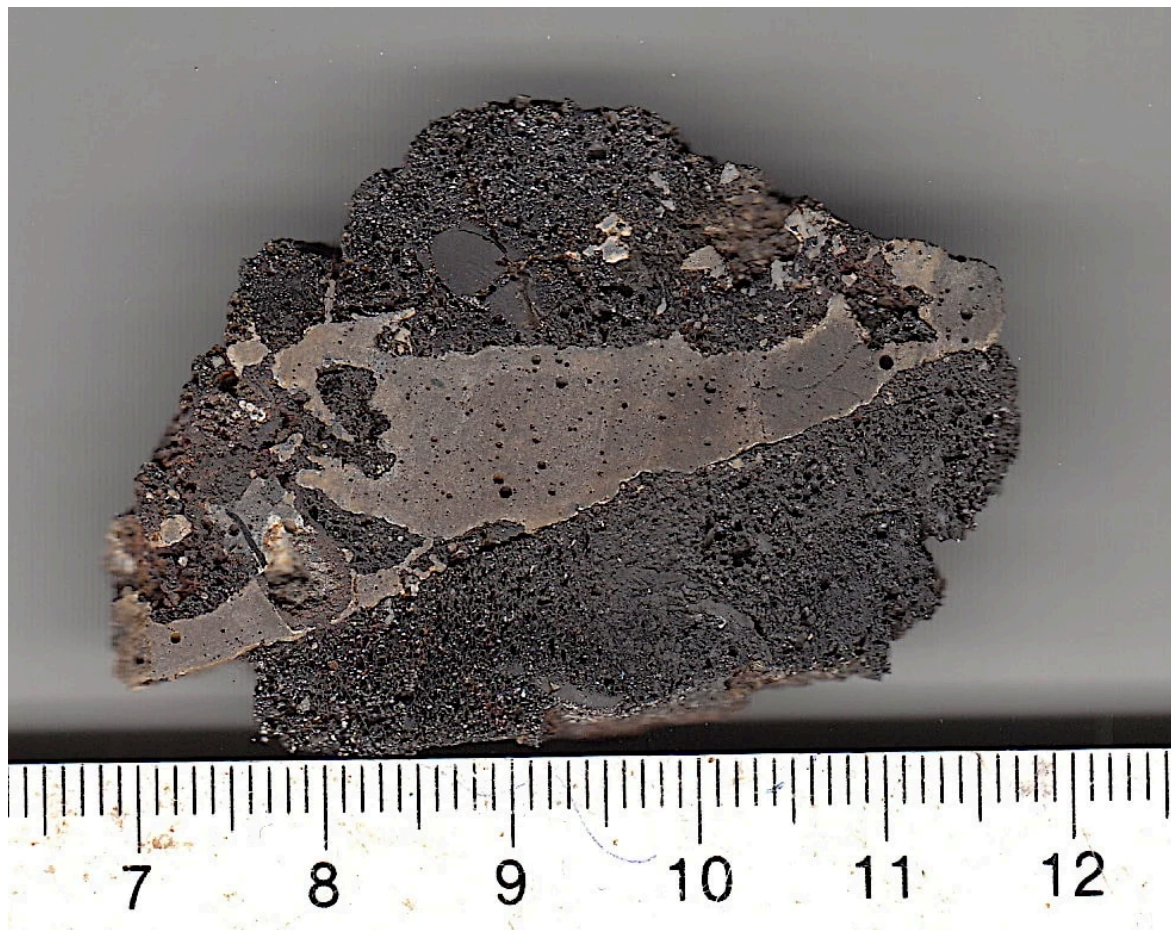
Larger black-glass melt rocks from new find locations, a few of which consisting of pure black glass. Coin diameter 22 mm.

Shatter cones



Shatter cone fracture markings in a big ejected quartzite block, proving impact cratering.

Chiemite

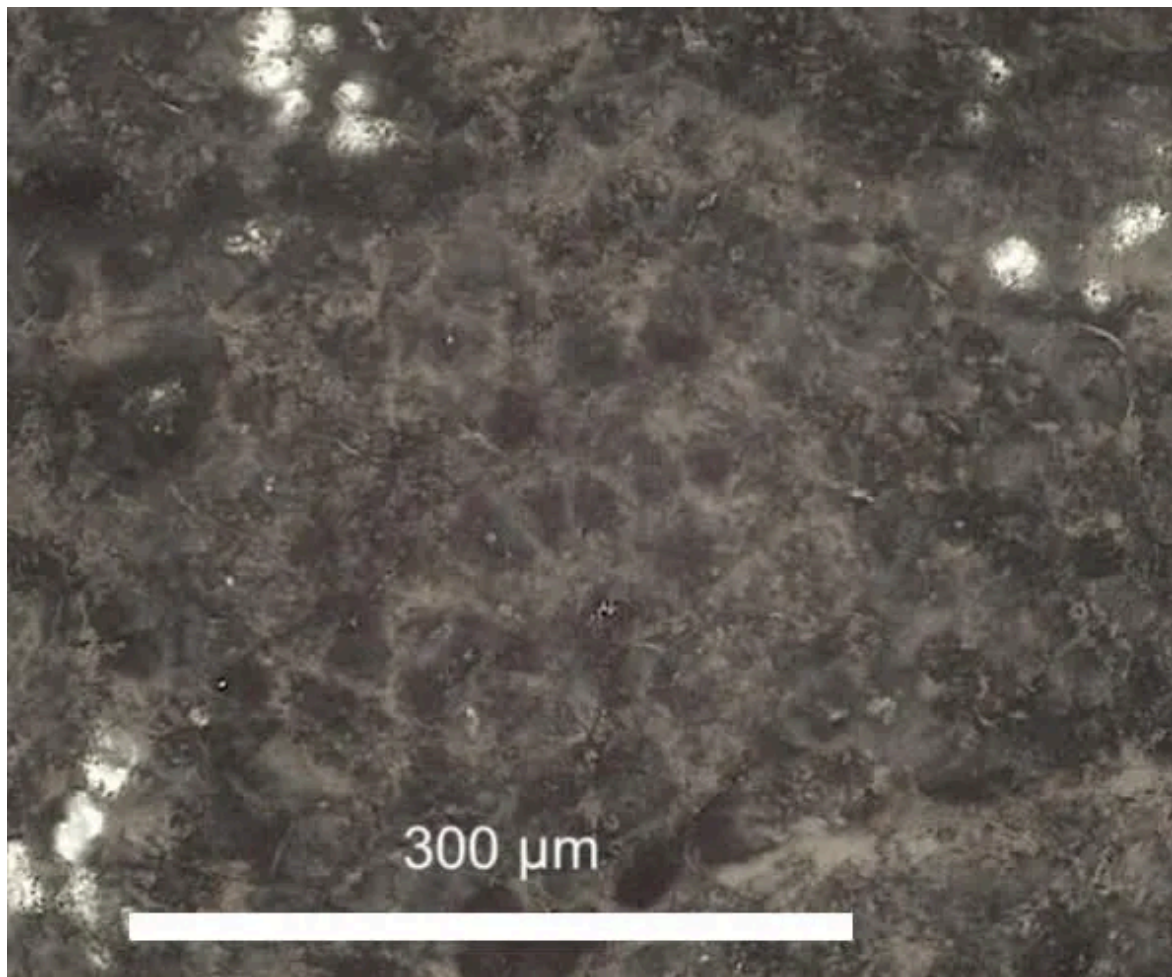


Chiemite, carbon impactite from strongly shocked vegetation. Top: Cut of cobble with an interlocking of chiemite with a fused vesicular sandstone, probably Triassic Muschelkalk sandstone. Siegel and Müller (2025).

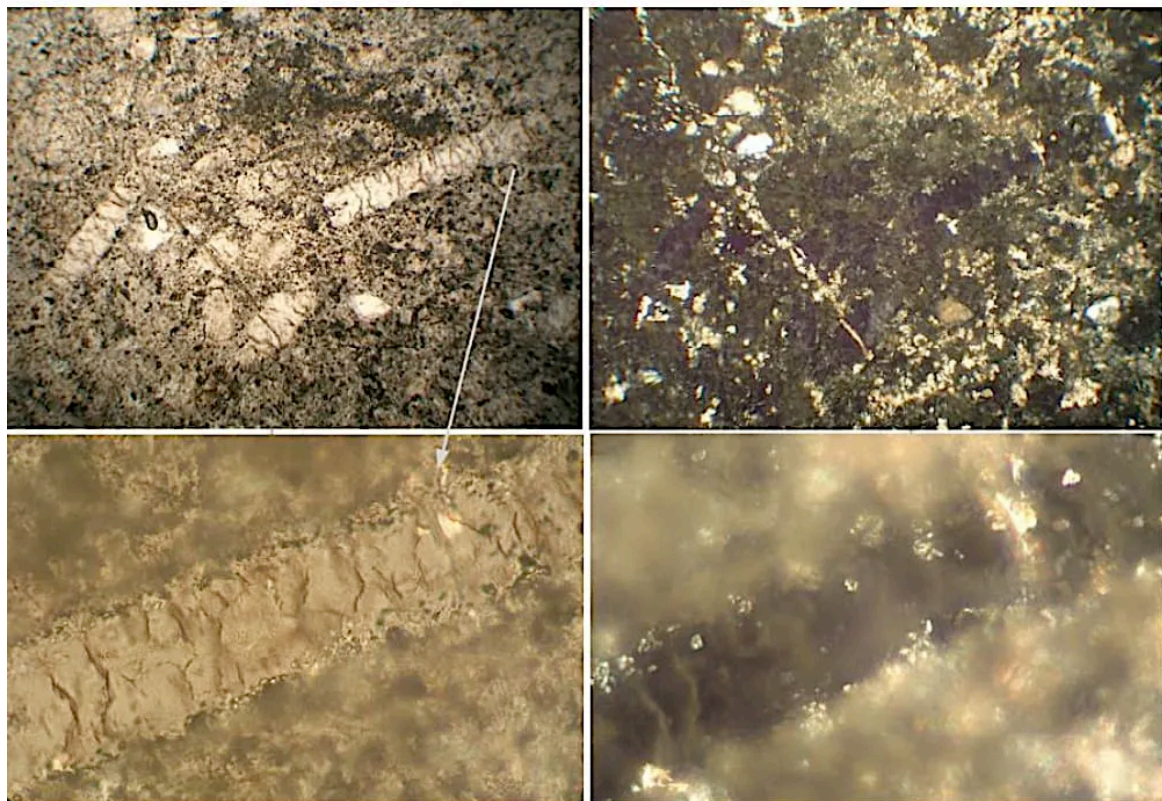
Shock metamorphism

Photomicrographs N. Berger, Thesis.

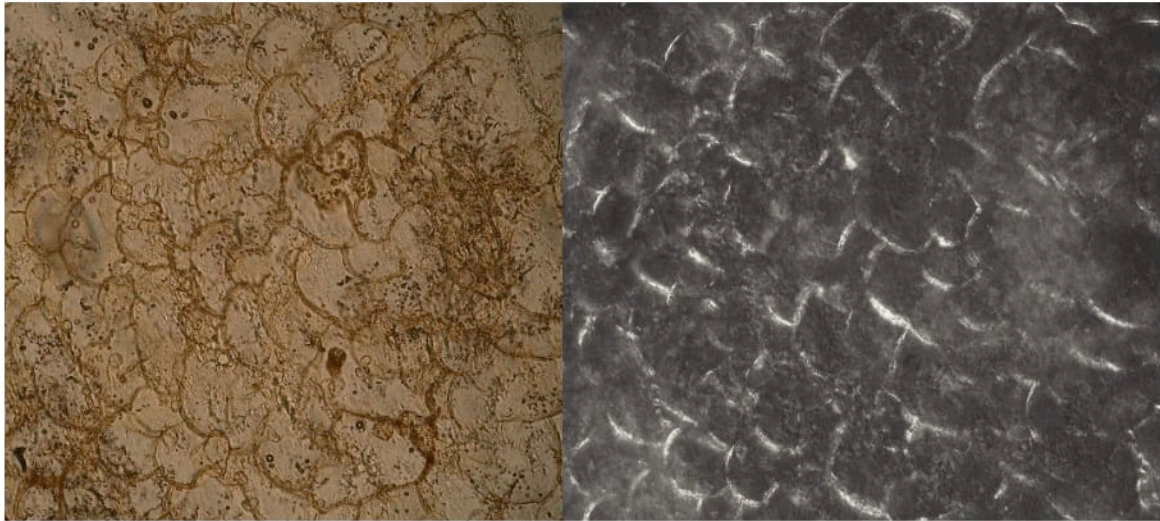




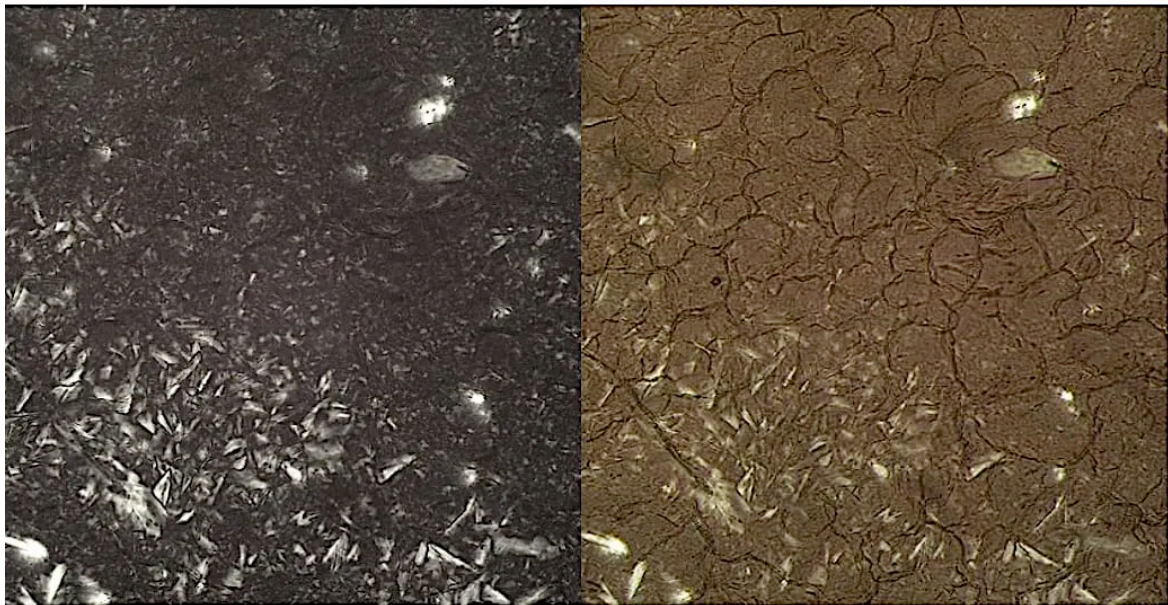
Shocked quartzite cobble transferred to diaplectic glass. Photomicrograph, PPL and crossed polarizers.



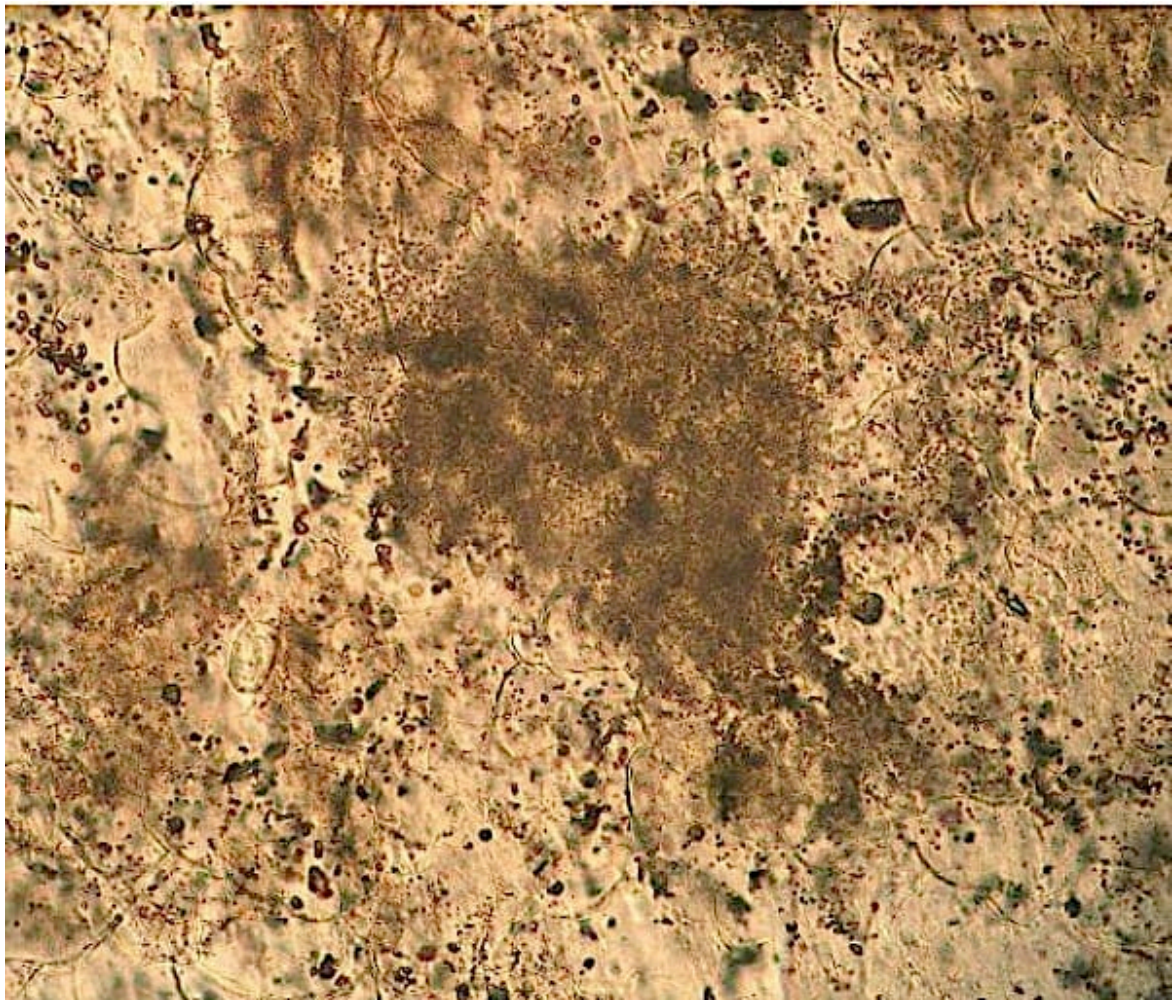
Shocked sanidine crystal in quartzite cobble transferred to diaplectic glass. PPL and crossed polarizer. Image width 560 μm.



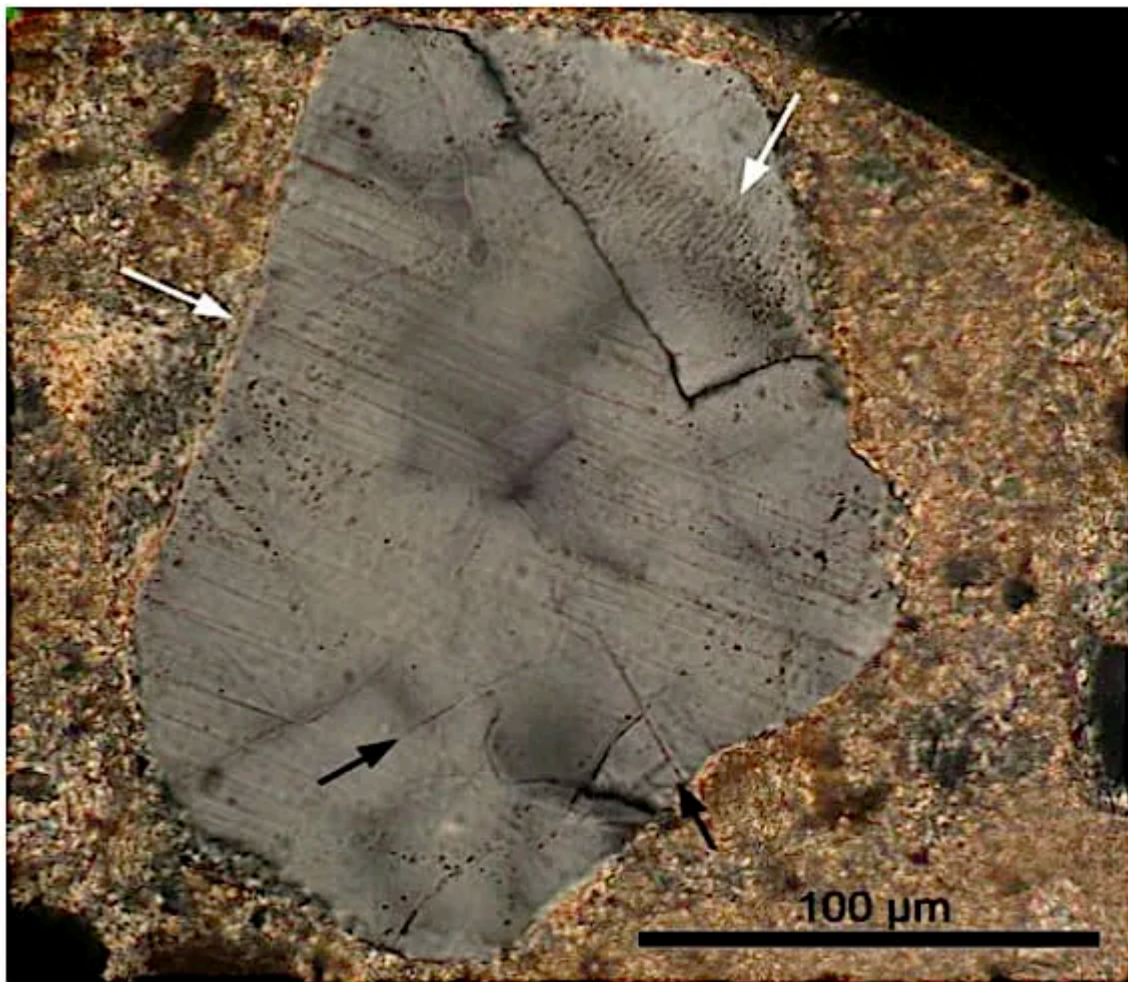
Blue glass with ballen structures; PPL and crossed polarizers, 560 μm image width.



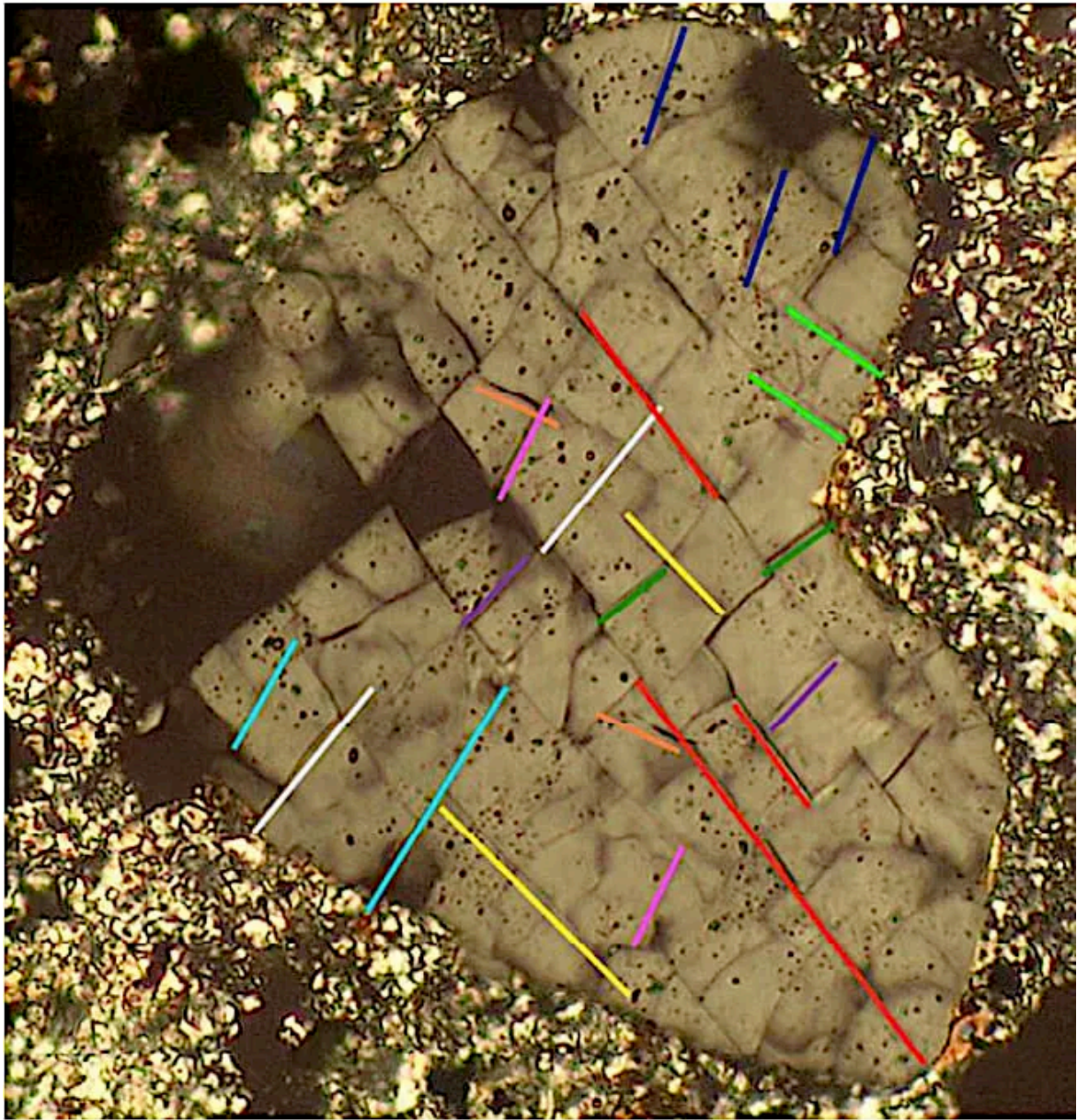
Ballen structures and cristobalite merging into tridymite. Crossed and slightly crossed polarizers. Image width 1.4 mm.



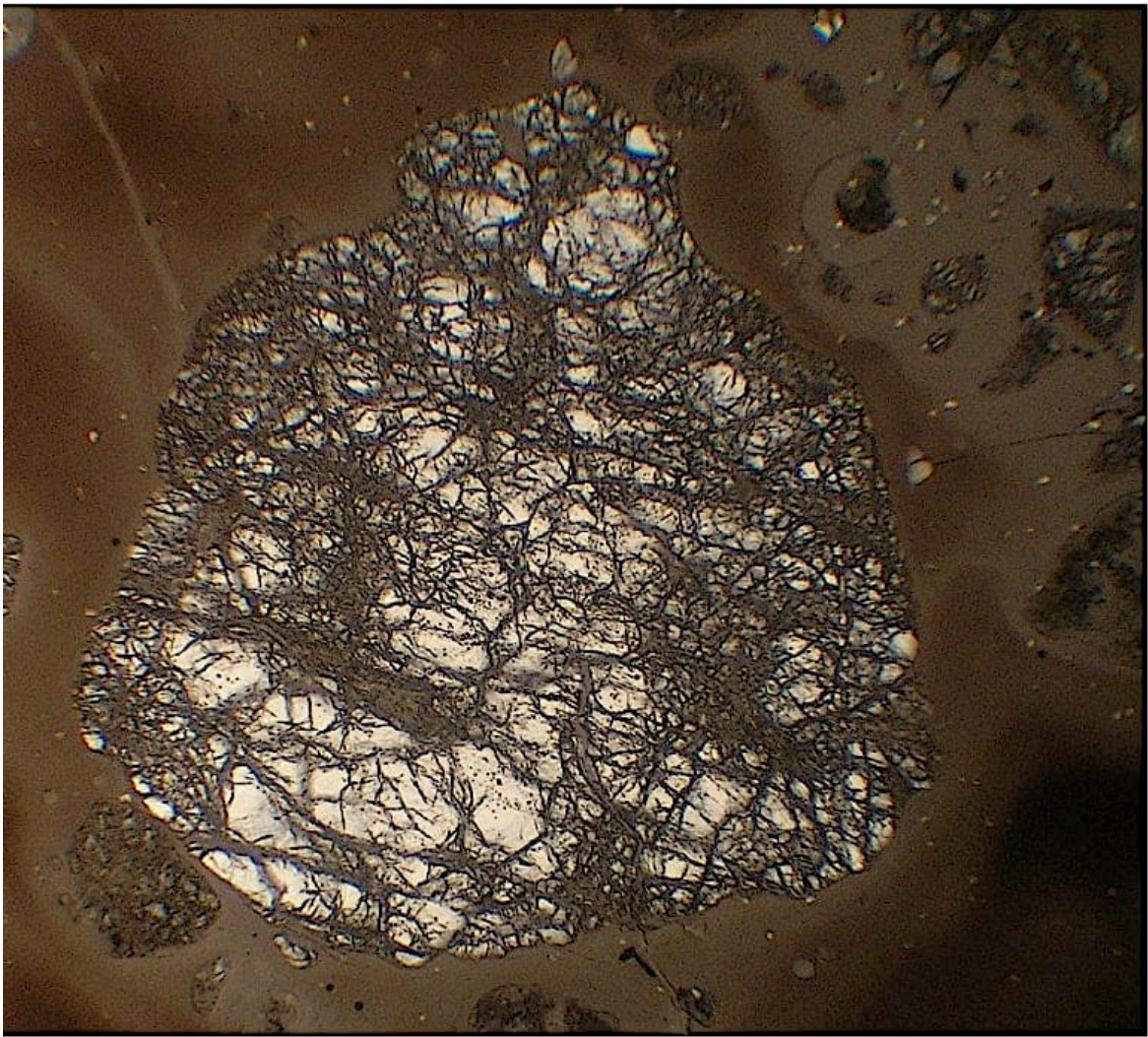
Toasted ballen quartz. PPL, 560 μm -



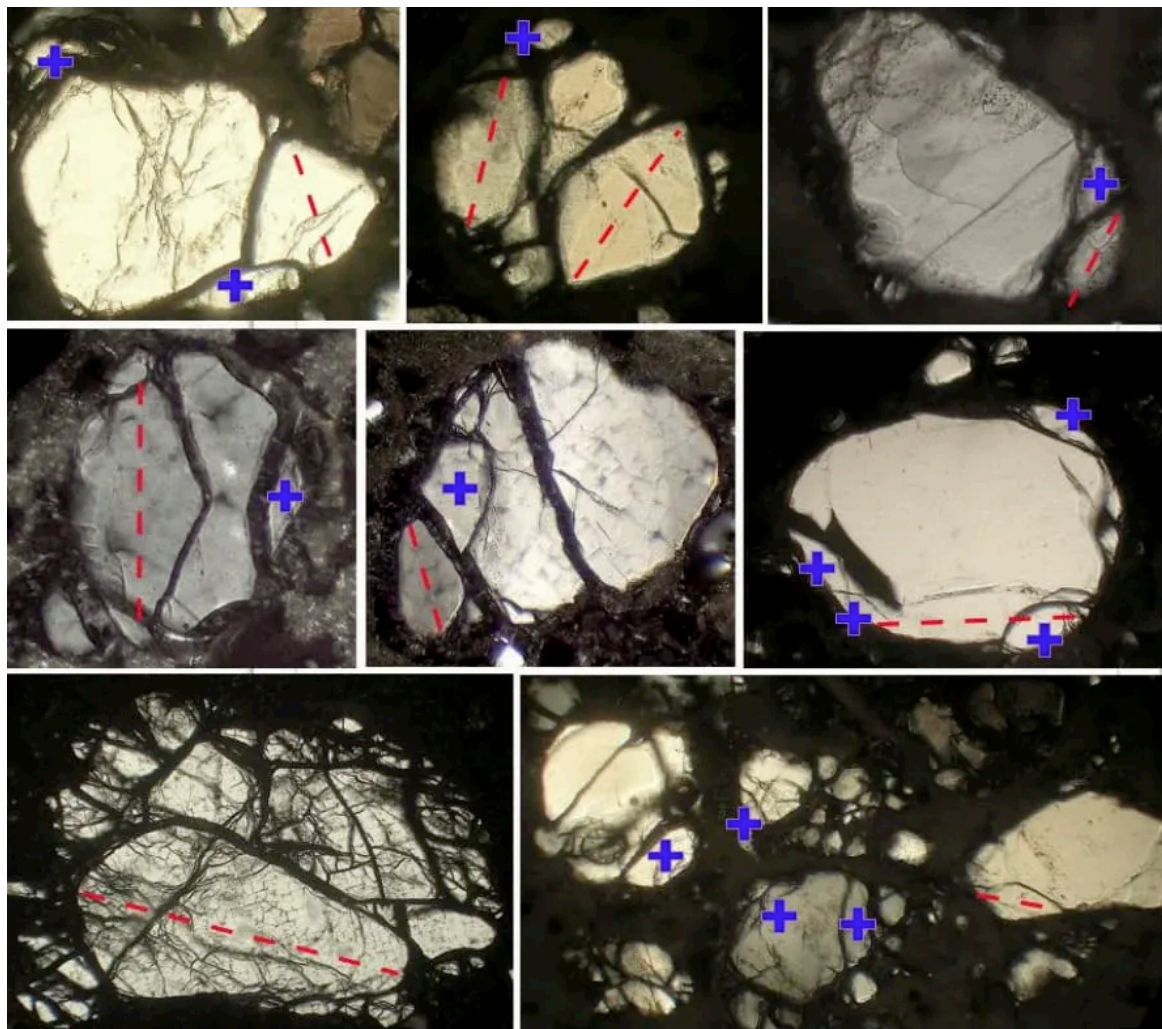
Two sets of planar deformation features PDFs (white arrows) and planar fractures PFs (black arrows) in quartz.



Quartz grain with a multitude of systems of planar fractures (PFs), in which uniform directions are marked in a uniform color; XX, image width 560 μm . Several fragments have been converted into diaplectic glass.

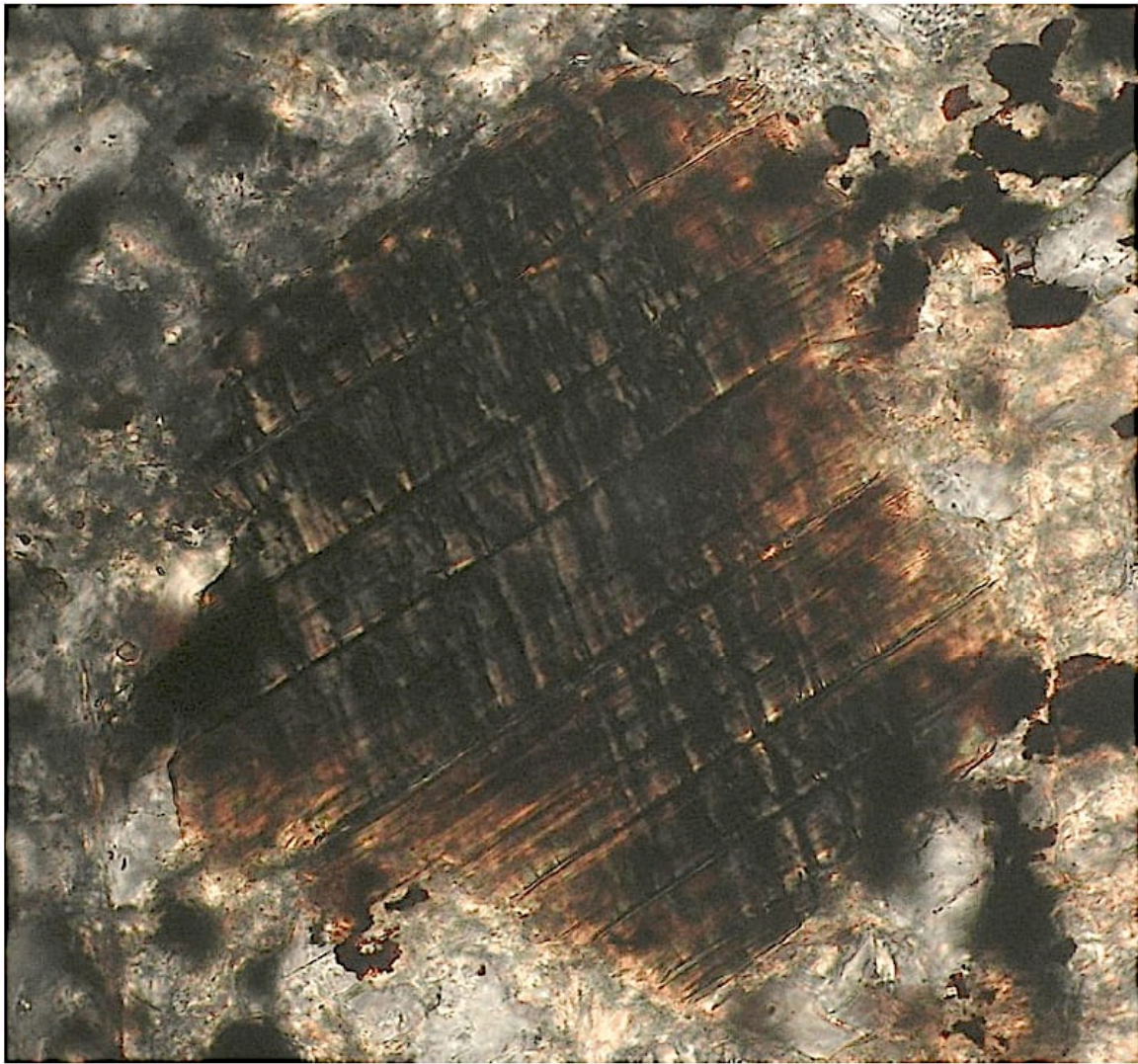


Finest fragmentation of a quartz grain with the fragments remaining cohesive; PPL; image width 3 mm.

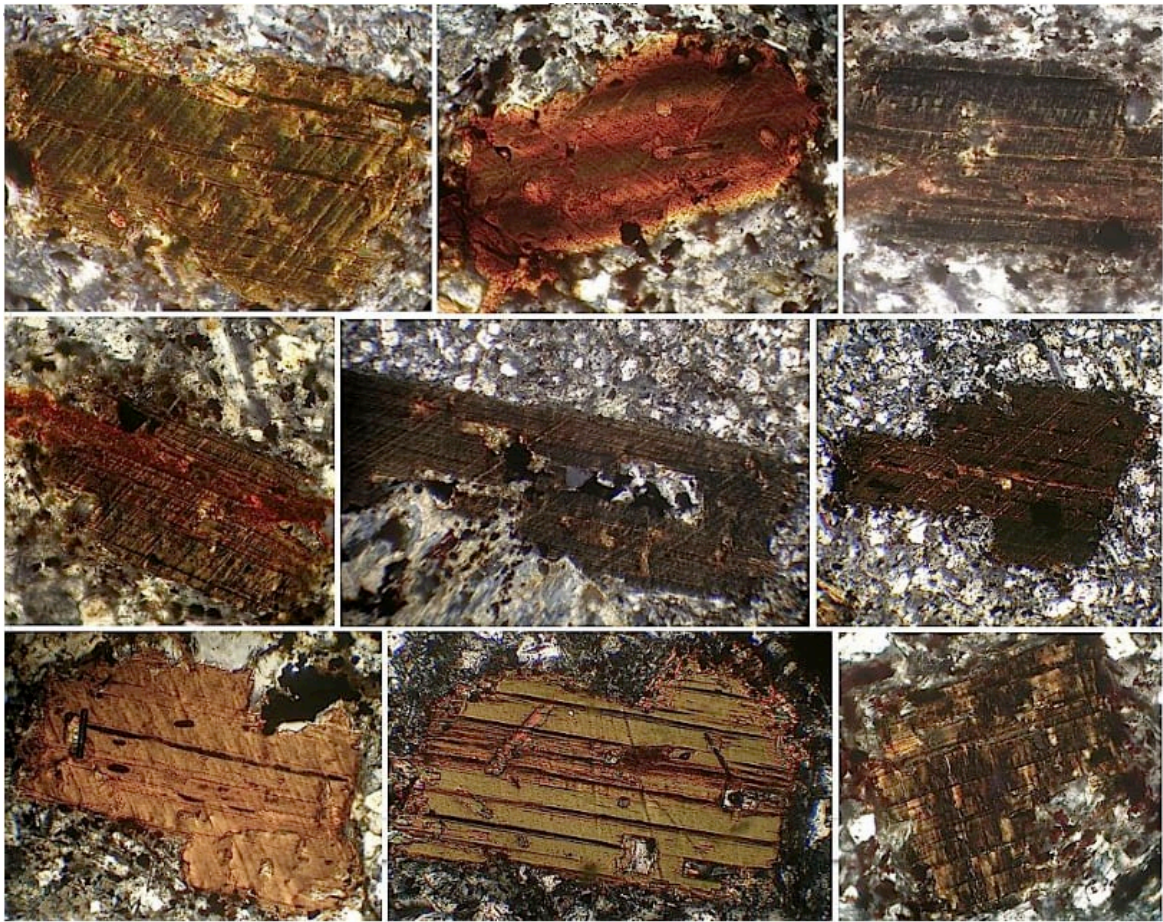


Compilation of quartz grains affected by shock spallation; PPL; image widths roughly 1.2 mm; blue: some marked “spalls”; red: symmetry lines within spallation fragments.





Mica grain (biotite) with intense kink banding (NNW – SSE) across the cleavage (SW – NE). XX, image width 750 μm .

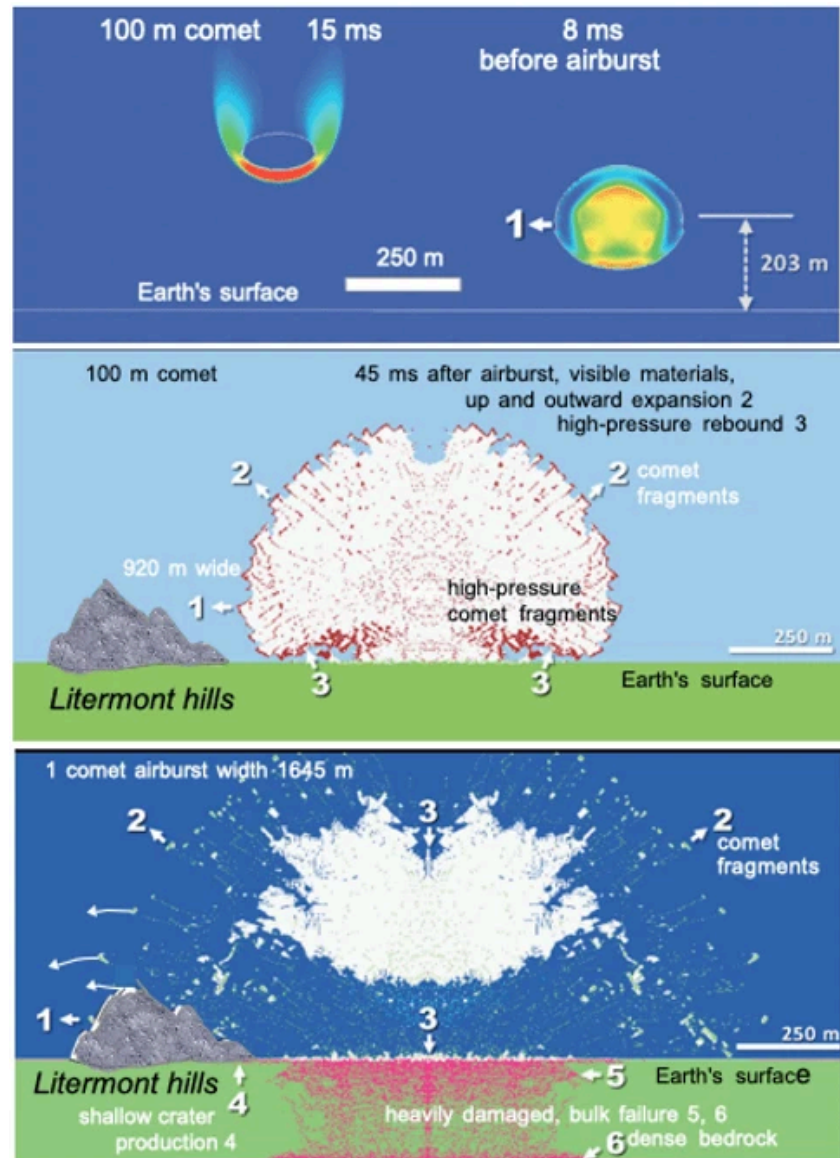


A compilation of micrographs that convey the diversity of planar deformation structures (PDFs) in biotites. The image widths are each about 0.5 mm

PRIMARY AND SECONDARY IMPACTS

Primary impacts

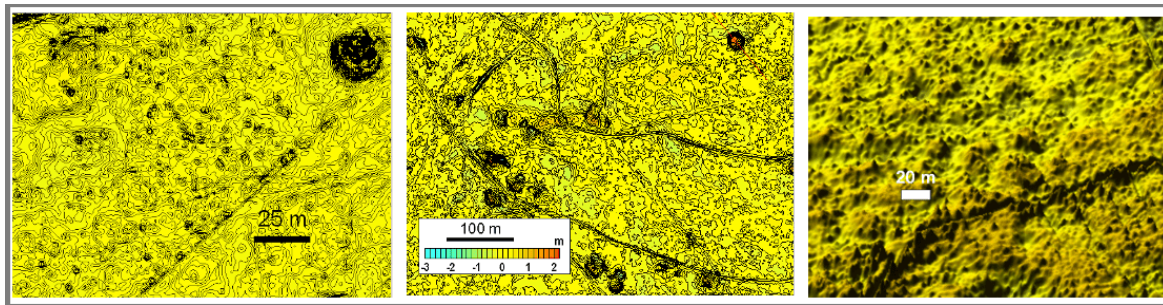
In impact cratering, the term secondary impact is used when (primary) ejecta, which have been hurled out at high energy, create (secondary) impact craters when they land.



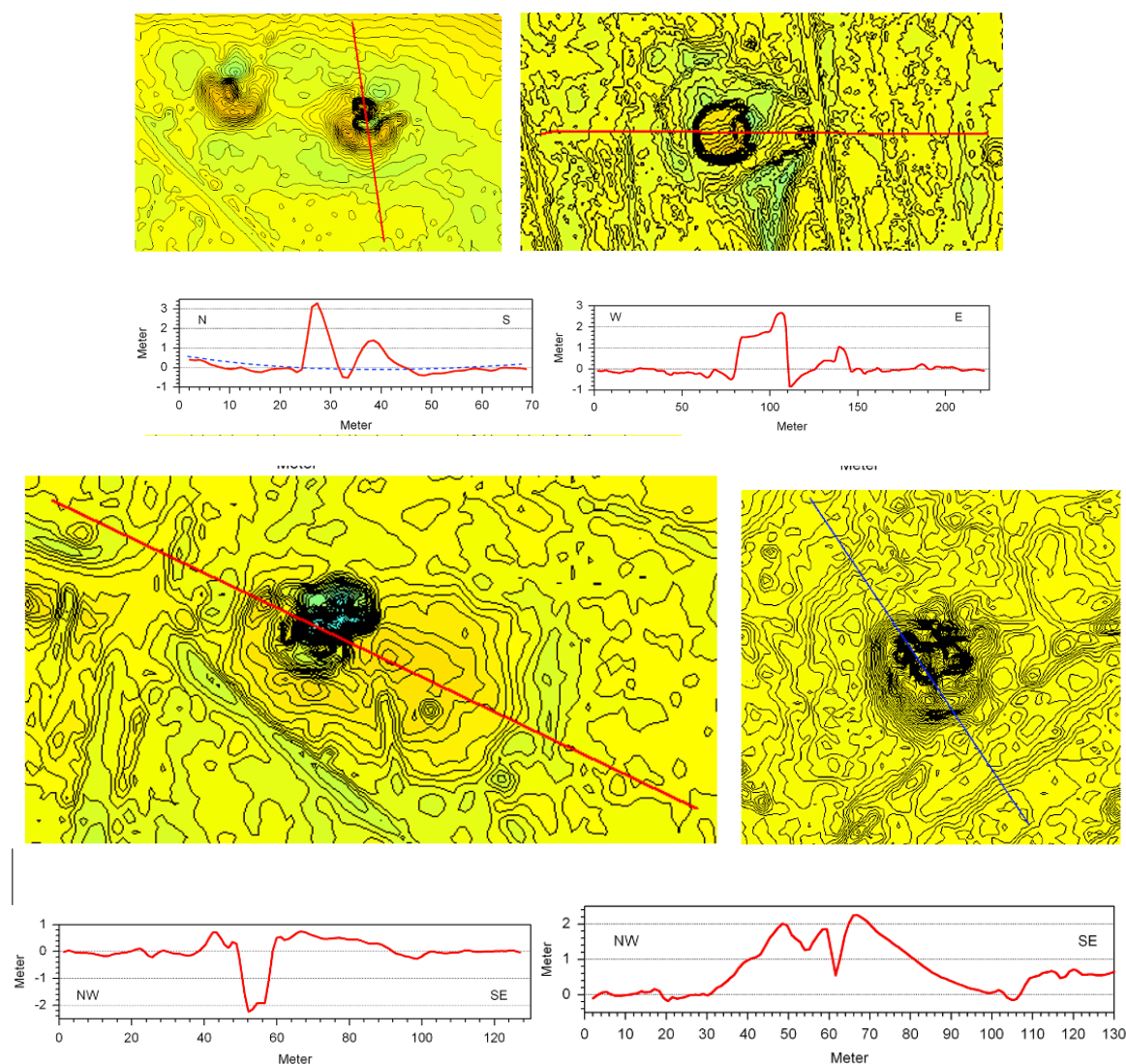
Hydrocode modeling of a comet low altitude touchdown impact airburst applied to the Saarland impact. Simplified and modified from West et al. (2024) [4].

In the present case of the Saarland impact with a postulated comet impact and a low-altitude touchdown airburst, it appears that we have a complex mixture of both primary and secondary impacts, which is entirely consistent with a complex comet composition, as discussed according to the latest findings in comet research. For the sake of simplicity, and because it is difficult to separate, we include here the structures caused by the exploded comet material among the primary impacts and those caused by the larger quartzite blocks thrown by the airburst from the Litermont among the secondary structures. Without knowledge of the terrain, the most difficult

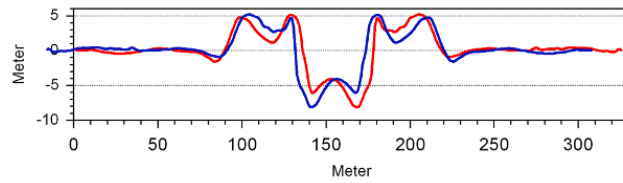
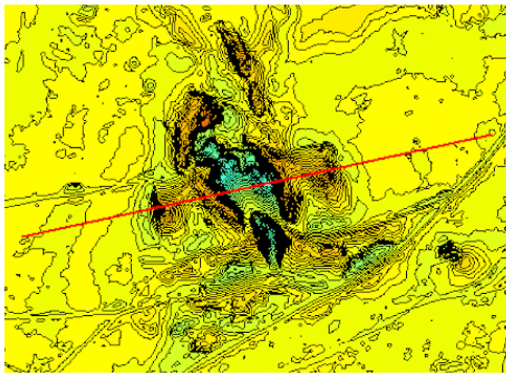
thing is to distinguish between the countless structures, presumably some 100, that may be sand boils caused by impact liquefaction (Ernstson and Poßkel 2024) but also quartzite blocks thrown away from the Littermont hills.



Sections of the selected impact area with the dense overprint of impacts spots.



DTM contour maps of primary impact structures, and DTM profiles. Contour intervals 5 cm - 20 cm.

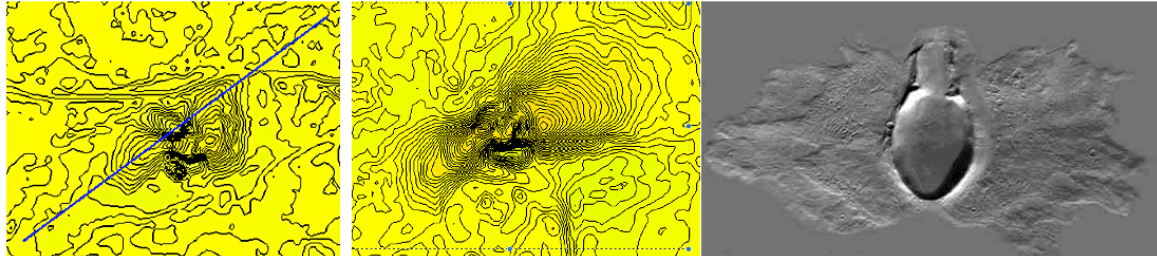


This example (out of many) demonstrates the important conclusion that this morphological feature can neither be geogenic nor anthropogenic. The central symmetry of the red and super-imposed mirrored blue profile shows deviations of no more than a few meters to decimeters over a length of 200 m, which can only be explained by a point source above the center.

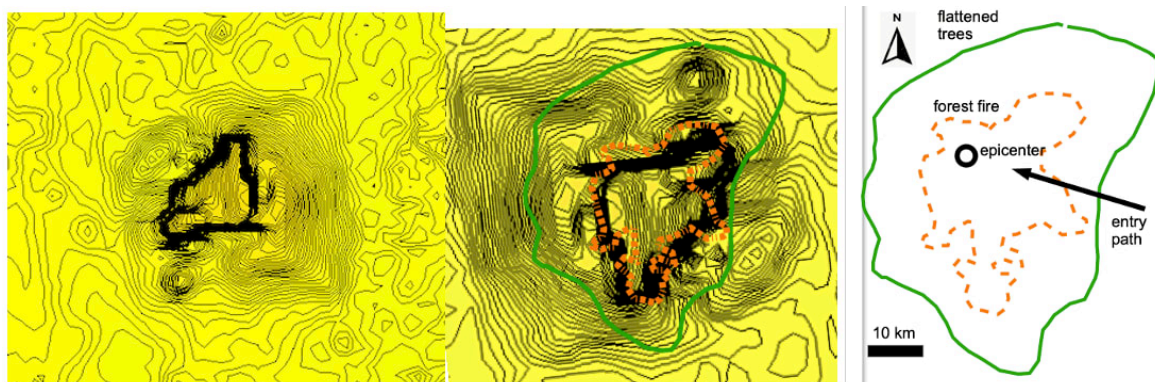
PRIMARY AND SECONDARY IMPACTS

Butterfly impacts.

Often, the impact structures have a kind of butterfly shape, which, although in very different sizes, are related to structures on Mars and at the Tunguska airburst impact (Figs. 6, 7). In the case of the Tunguska airburst, the geometrically similar shape is striking (Fig. 7), which indicates a similar energy distribution upon oblique entry.



Butterfly impacts: Saarland and Mars.



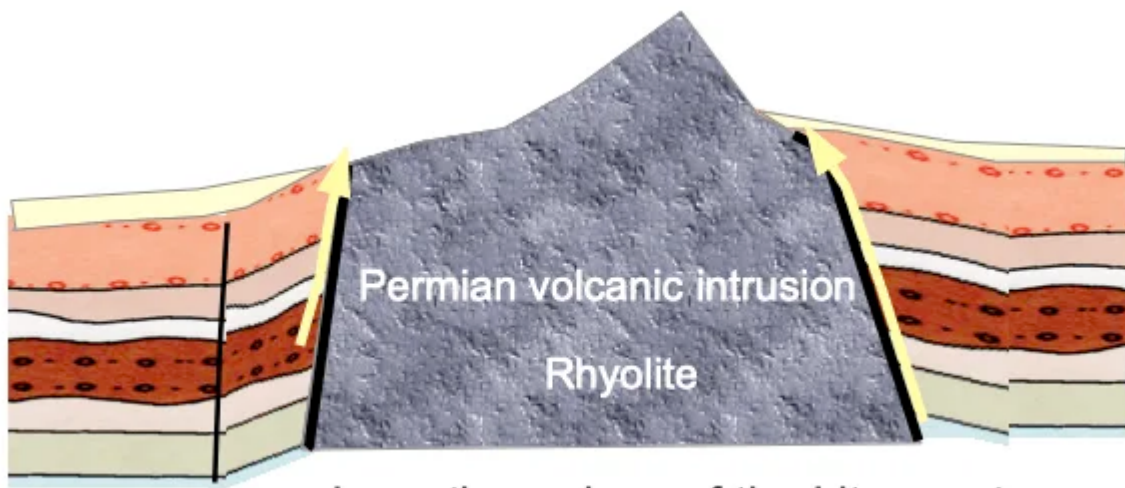
Butterfly impacts Saarland and Tunguska airburst (modified from [6]).

Secondary impacts

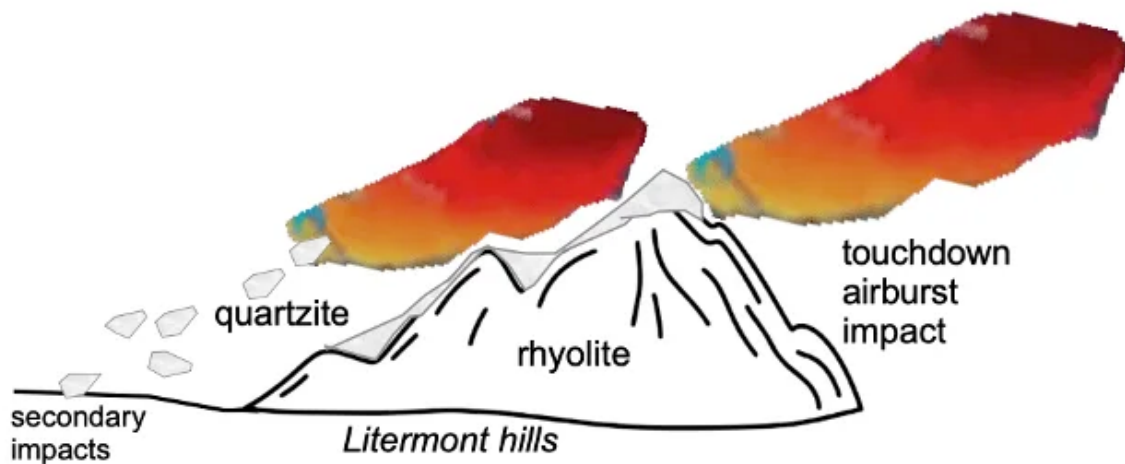
Here we focus on a limited selection of characteristic DTM examples, which as mentioned above, are assumed to morphologically reflect secondary impacts from emplaced quartzite rocks.



The Littermont elevation, a geologic benchmark in the impact event, which points to primary and secondary impact signatures.



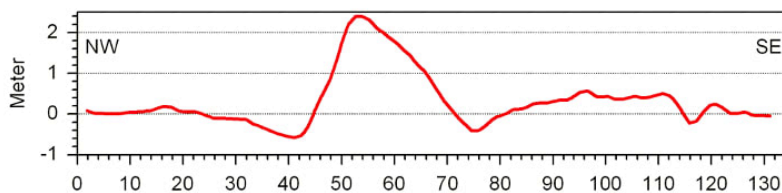
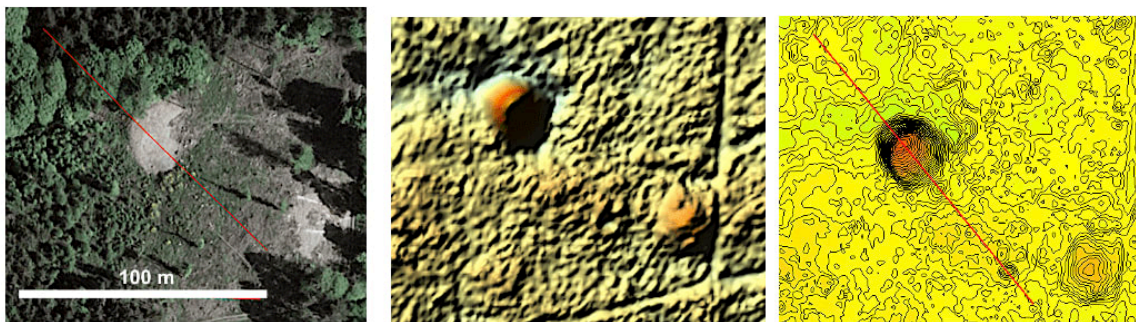
schematic geology of the Littermont



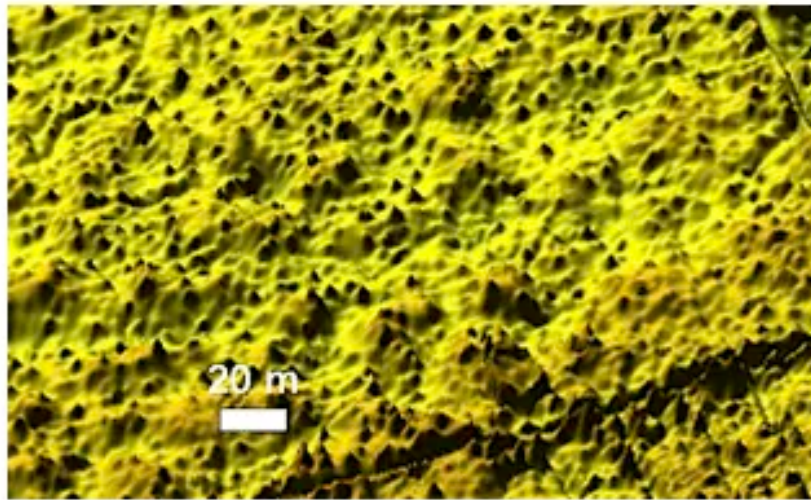
Sketch of secondary impacts: Airburst shattering and cutting back of the Littermont Hills quartzite top.



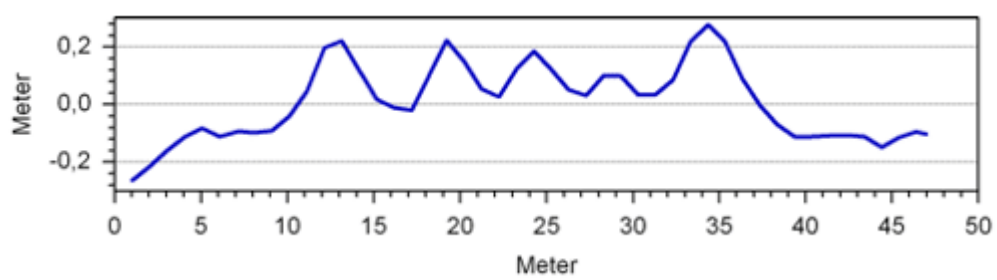
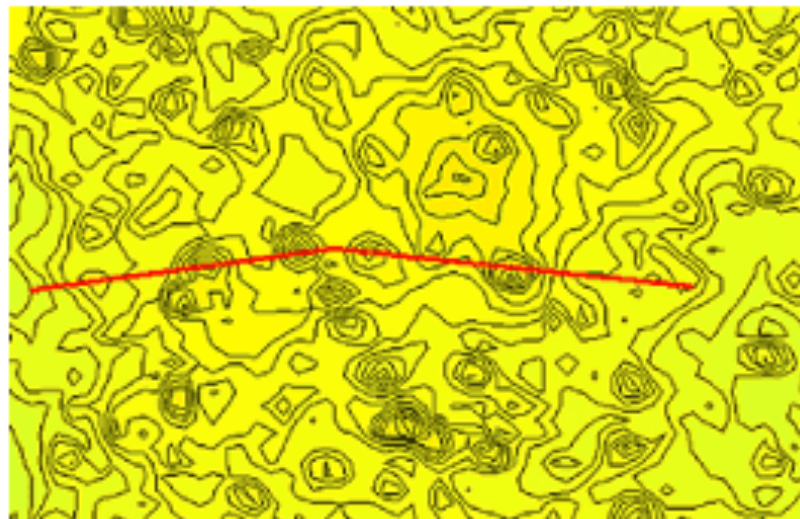
Allochthonous quartzite blocks that have landed over hundreds of meters as a long-distance ejection from the Littermont impact airburst "attack".



Google Earth image. Tree-free emplacement of quartzite blocks, and digital terrain model: 3D terrain surface, contour map (interval 10 cm) and topographic profile. A small, rimmed crater at the end of the profile.



Cluster of sand boils as DTM 3D.



Topographic contour map and DTM profile.

DISCUSSION

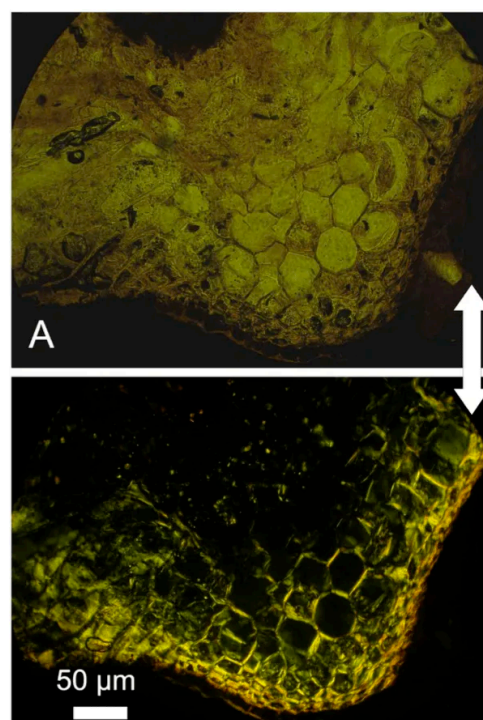
With the routine application of the extremely high-resolution digital terrain model (DTM), impact research has entered a new phase. What we have already referred to as an obvious paradigm shift (Ernstson et al. 2024 [5]) has hardly been adopted in traditional impact research or is deliberately ignored, which is not discussed here. As can be seen from the title, this development also applies to new findings on low-altitude touchdown airburst impacts, whereby there is undoubtedly a fruitful complementarity between the two, as already mentioned in the introduction.

The opinion that airburst impacts have posed a far greater threat to terrestrial civilization than point impacts at all times has been articulated earlier (e.g., Boslough and Crawford 2008 [7]), and recently there have been publications about fossil records of terrestrial airbursts in the form of spherule layers (van Ginneken et al. 2024 [8]). An important but ultimately controversial example of a touchdown airburst impact is the Libyan Desert Glass (LDG) (Kovaleva et al. 2023 [9], among others), which some authors still attribute to a point-shaped impact, the crater of which, however, has still not been found.

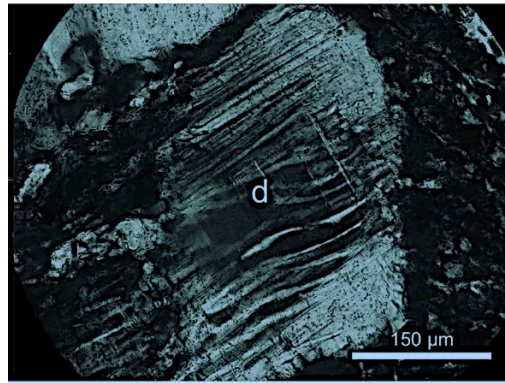
The latest argument in favor of this hypothesis is the detection of a zircon polymorph in an LDG sample, which can only have been created at very high shock pressures during a point-shaped, crater-forming impact. In the article by Cavosie and Koeberl (2019) [10], this is formulated as follows: “.... the two main formation hypotheses include melting by meteorite impact or melting by a large, 100 Mt–class airburst. High-temperature fusion occurs during both processes, however airbursts do not produce shocked minerals; airbursts generate overpressures at the level of thousands of pascals in the atmosphere, whereas crater-forming impacts generate shockwaves at the level of billions of pascals on the ground”.

And D. Stöffler writes: "Mineral glasses are formed by shock compression of silica or silicate minerals (single crystals or non-porous rocks) in the pressure range of about 25 to 55 GPa. Rock glasses (i.e. total rock melts) require peak pressures in excess of 60–80 GPa." (Stöffler 1984, online 2003).

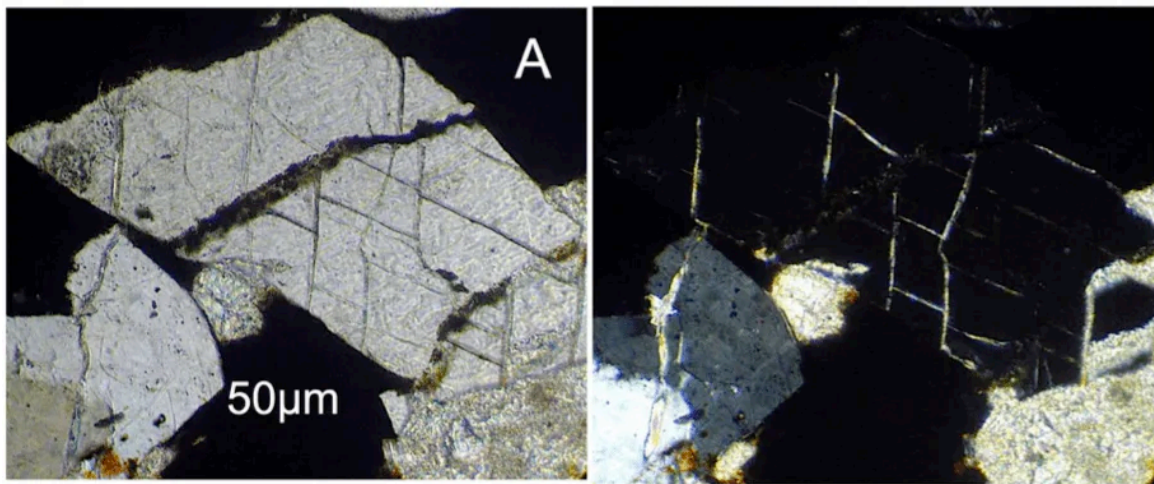
We compare:



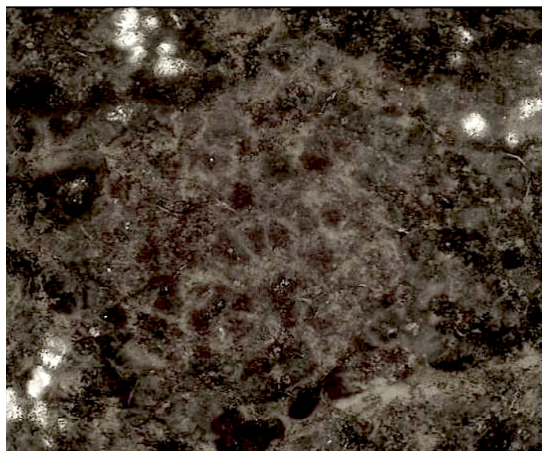
Czech Republic, touchdown airburst impact, diaplectic SiO₂ glass, PPL and crossed polarizers.



Chiemgau touchdown airburst impact, quartz PDFs merging into diaplectic glass; crossed polarizers.



Quartz grain completely transferred to diaplectic glass. The multiple sets of planar fractures PFs are also a shock effect. PPL and crossed polarizers.



Saarland impact, diaplectic quartz grain texture; crossed polarizers.

We compare the Cavosier and Koeberl claim with regularly occurring diaplectic glass from low altitude airburst impacts:

Holocene touchdown airburst impacts (above images), abundant diaplectic SiO₂ glass:

Czech impact strewn field

Chiemgau impact strewn field

Niederrhein impact strewn field

Saarland impact strewn field

Shock pressure 25 - 55 GPa

Zirkon polymorph ZrSiO₂ reidite formaton

Shock pressure 30 GPa

The conclusion: Cavosier and Koeberl are fundamentally wrong when they claim that airburst impacts do not produce shock effects at the ground and that the reidite in the LDG could only arise from a crater-forming impact. The airburst origin of the LDG is not questioned by Cavosier and Koeberl.

References

- [1] Ernstson, K. et al. (2013) 76th Ann. Met. Soc.Meeting, Abstract 5059.pdf. [2] Ernstson, K. et al. (2018) 49th LPSC, Abstract #1876. [3] Siegel, U. et al. (2022) 53rd LPSC, Abstract and Poster 1842.pdf. [4] West, A. et al. (2024) Airbursts and Cratering Impacts, 2(1). [5] Ernstson, K. and Poßekel, J. (2024) AGU24, Abstract and Poster EP01-29. [6] <https://www.nasa.gov/history/115-years-ago-the-tunguska-asteroid-impact-event>. [7] Boslough, M.B.E and Crawford, D.A. (2008) Inter. J. Impact Engineering, 35, 1441-1448. [8] van Ginneken, M. et al. (2024) Earth Planet. Sci. Let., 627, 118562. [9] Kovaleva, E. et al. (2023) American Mineralogist; 108 (10): 1906–1923. doi: <https://doi.org/10.2138/am-2022-8759>. [10] Cavsie, A.J. and Koeberl, C. (2019) Geology, 47, 609-612. [11] Stöffler, D. (1984) Journal of Non-Crystalline Solids, 67, Issues 1–3, 465-502.
-

TRANSCRIPT

